Molecular charge transport : relating orbital structures to the conductance properties

Guédon, C.M.

3

Nanoparticle array based strain sensor

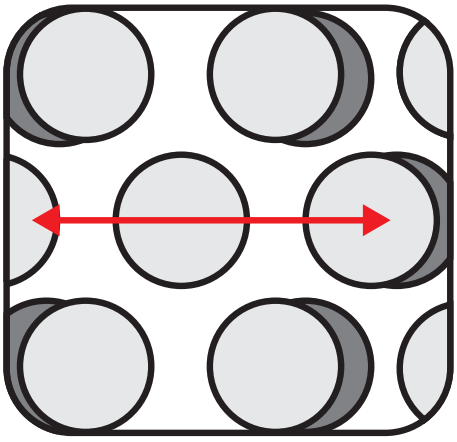

The results presented in this chapter have been published as:

C. M. Guédon, J. Zonneveld, H. Valkenier, J. C. Hummelen and S. J. van der Molen, *Controlling the interparticle distance in a 2D molecule-nanoparticle network*, **Nanotechnology**, **22**, 125205 (2011)

3.1 Introduction

Research in molecular electronics is strongly inspired by the possibility to encode a well-defined functionality, such as switchability, into a single molecule [1, 2]. On the road towards nanoscale functional devices, various fundamental questions arise. Many of these have to do with the details of the connection between a molecule and two electrodes. For example, the distance between the electrodes defines if and how a molecule can be connected between two metals. Moreover, a molecule that exhibits a significant length change upon switching is likely to lose its functionality in a rigid junction. Interestingly, the inverse may also be true, a possible example being spin transition molecules [3]. Since the length of such a molecule is larger in its high-spin than in its low-spin state, straining it may actually induce a spin transition.

Here, we aim for a stable molecular device structure which allows one to vary the inter-electrode distance on the sub-Ångstrom scale. For this, we combine two techniques which have proven their use in molecular transport studies: mechanically controllable break junctions (MCBJ) [4, 5], and 2D nanoparticle-molecule networks[6–9]. MCBJs are widely used to study single molecule conductance and allow for tuning of the inter-electrode distance with great accuracy. However, they lack stability at room temperature. Devices based on molecule-nanoparticle networks, on the other hand, offer great stability even at 293 K. One reason for this is that a nanoparticle-molecule-nanoparticle junction has a tiny mechanical loop. The other reason is that a conductance measurement forms a statistical average over a full array. Hence, fluctuations (molecular bond breaking and re-attachment) on the single junction level average out. Here, we combine the advantages of both techniques to create a 2D molecule-nanoparticle network in which the interparticle distance can be varied.

3.2 Experimental details

We start with the synthesis of gold nanoparticles (NP's) following the Slot and Geuze method [10]. In this way we obtain NP's that are 10 ± 1nm in diameter and charge stabilized in water. Next a solvent exchange step is performed (water to ethanol) to self-assemble alkanemonothiols, in this case octanethiols, on the NP's to prevent aggregation. After another solvent exchange step (ethanol to chloroform) the NP's are self-assembled into a 2D network on a convex air-water interface due to the evaporation of the solvent. This is followed by a microcontact printing step, i.e., the network is transfered from the water surface to the substrate using a polydimethylsyloxane (PDMS) stamp. Note that the self-assembled alkanethiols define the initial inter-particle distance[7]. As a bendable substrate, we use phosphor bronze which needs to be electroni-

cally isolated from the NP's. The insulating layer applied will also need to transmit the substrate deformation and to offer good adhesion to the NP network. We tested four different materials (PMMA, N-1410, SU-8 and poly-imide) spin coated on our substrates. Poly-imide, already used for MCBJ substrates [4, 11], shows the best adhesion properties for the NP's. Finally gold contacts are deposited by shadow mask evaporation, the electrodes being 160 μm apart. In this way, a network is created in which a unit junction comprises two nanoparticles separated by a tunnel barrier that consists of two monolayers of alkanemonothiols. From here it is also possible to create a 2D network of metal-molecule-metal junctions using a place exchange step[6–9]. This results in the formation of one or a few molecular junctions as discussed below (see also chapter 2). Interestingly, the network's sheet resistance can be directly related to the average resistance of a single junction [7](chapter 2).

For our experiments, we mount a substrate onto a MCBJ set-up, as illustrated in figure 3.1-A. A pushing rod, capable of bending the substrate in a three-point geometry, is driven by a motor that can be operated continuously or stepwise. The network on the substrate is connected via spring-loaded contacts to an IV-converter and a data acquisition card. A bias voltage of 2V is typically applied to the network, resulting in a voltage drop of a few mV for each junction. The resistance is recorded while bending. All the measurements are done at room temperature and in a low vacuum chamber at a pressure of about 10^{-3} mbar.

3.3 Results: bending the network

Let us first anticipate what happens when we bend a network with alkanemonothiols only, i.e. without dithiolated molecular bridges. When displacing the pushing rod by a distance Δy, as shown in figure 3.1A, the upper surface of the phosphor bronze substrate is elongated. Its deformation is transmitted by the poly-imide layer to the NP network (figure 3.1B), resulting in lateral strain on the network. To get a picture of the resulting resistance behavior of our structure, we note that a unit junction formed by two NP's is basically a tunnel junction. Its barrier height, φ, is defined by the work function of gold covered by alkanemonothiols. The barrier width is the distance d between the edge of two NP's as shown in figure 3.1C. For reasons becoming clear later, we also define u, the distance between the centers of the two nanospheres. The junction resistance can be written in the form: $R \propto e^{2\kappa d}$ where $\kappa = \frac{1}{\hbar}\sqrt{2m\varphi}$ with m the electron mass and $\hbar$ the reduced Planck constant. The change in resistance when elongating the junction with Δd is thus

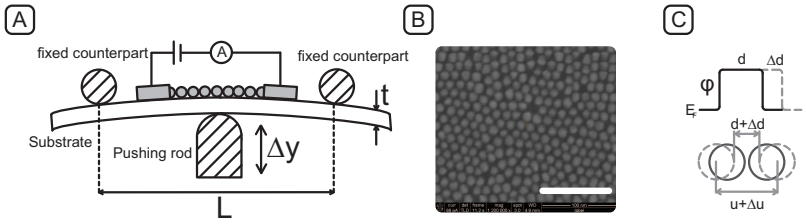

FIGURE 3.1: **Overview of the experimental details. A** Schematic cross-section of the measurement set-up. By bending a phosphor-bronze substrate in a three-point geometry, a 2D nanoparticle-molecule network is stretched. **B** Scanning electron micrograph of an octanemonothiol protected gold NP network; the scale bar shown is 100 nm. **C** Schematic view of the tunnel barrier when the distance between the surface of two nanoparticles is increased from d to d+Δd. We define u as the distance between the centers of the nanoparticles. Note that $\Delta u = \Delta d$. The height of the energy barrier equals φ.

expected to follow: $ln(R(\Delta d)/R(0)) = 2\kappa\Delta d$, where $R(0) \equiv R(\Delta d = 0)$. In the linear regime we can simplify this relation to: $(R(\Delta d) - R(0))/R(0) = 2\kappa\Delta d$. Hence, we can accurately monitor the displacement between the nanoparticles by measuring the network's resistance response.

In a typical experiment the substrate is bent back and forth by moving the pushing rod in steps of $\Delta y = 0.043$ mm. After each step the resistance change is probed. Figure 3.2 shows the result for a sample with octanemonothiol tunnel junctions with an initial resistance of 176 $M\Omega$. The data are plotted both linearly, showing $(R(\Delta d) - R(0))/R(0)$ vs Δy, and semi-logarithmically, displaying $\ln(R(\Delta d)/R(0))$ (see inset). Two experiments are shown; in the first case (black squares) the sample was bent less than in the second case (grey diamonds, also later in time). Figure 3.2 exhibits a plateau for small displacements. This has a trivial reason, as it corresponds to the situation where the pushing rod is not yet touching the substrate (see right bottom cartoon in figure 3.2). Once the substrate is actually bent, however, the resistance increases significantly, as anticipated above. For larger displacements, the curves deviate from linearity as indeed expected. Upon plotting $R(\Delta d)/R(0)$ semi-logarithmically, the curves become straighter. However a small deviation at high Δy is still present, probably due to plastic deformation (see below). As also can be seen on the other measurements in the supporting information we remain generally within the linear regime. The relative change in resistance $(R(\Delta d) - R(0))/R(0)$ per mm

pushing rod displacement for this sample is found to be 0.34 ± 0.02 mm^{-1} (from the black squares). We investigated five such samples and $(R(\Delta d) - R(0))/R(0)$ varied from 0.20 to 0.36 per mm pushing rod displacement, with an average of 0.30 mm^{-1}.

Let us now have a closer look at figure 3.2 and focus on the second experiment shown (grey diamonds) where the substrate is bent further than before, i.e. to Δy = 1.25 mm. In this case, the retracting trace does not come back to its original value. In fact, the plateau for small Δy, discussed above, is located at a higher resistance value and spans to higher Δy than before. This discrepancy is related to plastic deformation, i.e. permanent bending of the substrate as indicated in the left cartoon in figure 3.2. Hence, the pushing rod needs to move further up, to larger Δy, before additional bending is possible. All these observations demonstrate that the resistance change is due to network elongation, which itself results from deformation of the substrate. Hence, our device opens the road towards a strain sensor (or bending sensor) based on tunneling transport. In addition, we can deduce that the networks are more or less homogeneously deformed, i.e., deformation does not lead to fractures in the structure. Indeed, if fractures were formed, they would lead to large tunnel gaps and resistance increases much beyond our experimental results (see below). Furthermore, scanning electron microscopy (SEM) characterization after the bending experiment shows no evidence of fracture formation. We note that similar networks have been shown to be elastically deformable, with a Young's modulus of several GPa [12].

3.4 Analysis: How does the network deform?

Let us now have a more quantitative look at the deformation of the NP network and the resulting resistance changes. For this, we can rely on previous deformation calculations performed for MCBJs [4, 11]. When displacing the pushing rod by a distance Δy, the network will elongate by a distance ΔU, measured from electrode to electrode, as given by:

$$\Delta U = \frac{6tU\Delta y}{L^2}\zeta \tag{3.1}$$

Here L is the distance between the two fixed counterparts (20 mm in our case), t the thickness of the substrate (3 mm) and U the distance between the two evaporated electrodes (see figure 3.1) [4].

The correction factor ζ has been introduced by Vrouwe *et al.* to compensate for device-specific features such as undercut as well as stacking order of the different materials used [11]. In the ideal case where the deformation of the

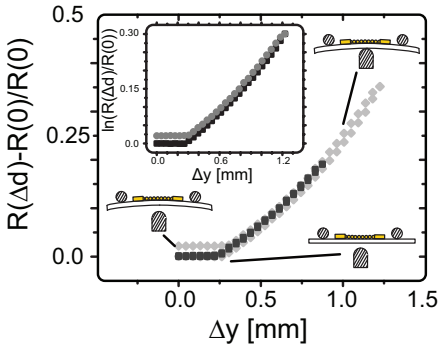

FIGURE 3.2: Relative resistance change as a function of pushing rod displacement, Δy. A schematic view of the substrate is shown next to the curve to illustrate: (i) the plateau for low displacements before the pushing rod touches the substrate, (ii) the case when the substrate is fully bent and (iii) hysteresis due to plastic deformation of the substrate. In the inset the same data is plotted in a semi-logarithmic way.

substrate is exactly transferred to the structure on top of it (MCBJ or network) $\zeta = 1$. In the case of lithographically defined MCBJ's the undercut amplifies the deformation of the substrate which results in $\zeta > 1$ [11].

The conductance through a NP network can be described from a simple unit cell as shown in figure 3.3 (see also chapter 2). Such a unit cell may be deformed in two ways. On the one hand, we consider the case where the NP's are well attached to the underlying layer. Then, the network will be deformed uniaxially as shown schematically in figure 3.3-A. On the other hand in figure 3.3-B we show the case where the NP's are loosely connected to the substrate. Then the network, when elongated in one direction, will be compressed in the perpendicular direction to keep its total surface constant; the so called Poisson effect. Let us define $N = U/u$ as the average number of nanoparticles between the electrodes in the $\hat{x}$ (or $\hat{u}$) direction. Consequently, for a network lattice direction lined up with the $\hat{x}$ direction $\Delta U = N\Delta u = N\Delta d$ (see figure 3.3). We can also calculate the length changes of the junctions in the other lattice directions, for both 2D-models, using simple trigonometry. With this we can obtain values for 2κ from the data for both 2D models. Let us first assume ideal transfer of deformation, i.e., $\zeta = 1$. The apparent 2κ values thus obtained in our experiments are 0.15 Å^{-1} for well attached NP's and 0.21 Å^{-1} for loosely connected NP's. These should be compared to a 2κ value of 0.87 Å^{-1} as experimentally found for alkanemonothiols in similar junctions [13]. We relate the discrepancy

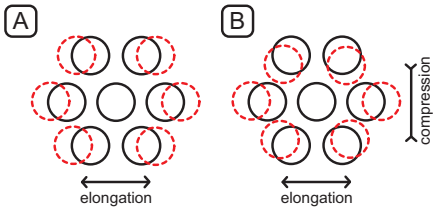

FIGURE 3.3: Schematic view of a basic lattice unit unstretched (black lines) and stretched (dotted lines). **A** The deformation is unidirectional as the NP's are well attached to the substrate. **B** As a consequence of the loosely attached NP's to the substrate the Poisson effect induces a compression in the direction perpendicular to the deformation.

to the incomplete translation of the substrate elongation to the network, i.e. to ζ being smaller than unity. Demanding that $2\kappa = 0.87\text{Å}^{-1}$ for our junctions as well, we find $\zeta = 0.18$ for uniaxially deformed networks and $\zeta = 0.24$ for Poisson deformed networks (full Poisson effect). There are several factors that may lead to a value $\zeta < 1$. Possibly, the polyimide layer takes up part of the deformation (unlike in MCBJ's there are no undercuts in our networks). However, our 2D NP array is also not perfect. It consist of many 2D-grains with a distribution of lattice directions. We tested our 2D-models for unit cells with different orientations, but found only small variations in ζ (up to 15 %). However, the grain boundaries may take up some of the strain. We note nevertheless that it is unlikely that the grain boundaries incorporate all elongation, since then a gap much larger than Δd would open. That would induce much larger resistance changes than we observe, due to the exponential nature of tunneling.

3.5 BENDING WITH BRIDGE-MOLECULES

As we have seen that a NP network can be controllably stretched, we can insert conjugated molecular bridges into it and study the response to deformation. For this, we choose acetyl protected dithiolated oligo-phenylene ethynylene molecules with three phenyl rings, i.e. OPE3. These are conjugated rod-like molecules (see lower inset of figure 3.4) that have been studied by several groups [7, 14]. The alkanemonothiol-protected gold NP networks are immersed in a 0.5 mM OPE3 solution, deprotected by triethylamine in tetrahydrofurane (THF), for 24 hours[15]. This allows the dithiolated OPE3 molecules to form bridges between two neighboring NPs, as indicated in the inset of figure 3.4 [7, 8]. (However, as we discussed in chapter 2, there is no conclusive proof of the

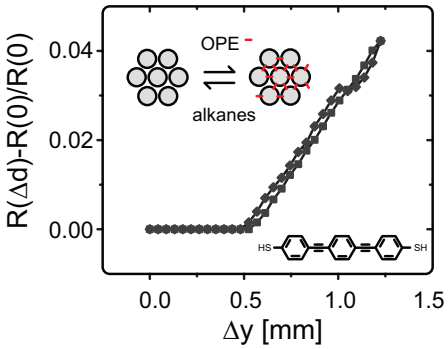

FIGURE 3.4: **Bending a network with OPE3-bridges.** Relative resistance change as a function of pushing rod displacement for a network with OPE3-bridges. The pushing trace is represented by squares and the backward trace features diamonds. In the upper inset the molecular exchange reaction is schematically depicted and in the lower inset the chemical structure of OPE3 is shown. Note the kink in the back trace around 1 mm, which is due to slipping of the driving motor

molecules fully bridging the nanoparticles.) After this procedure, the resistance of the network in figure 3.2 has dropped to 34 MΩ, as compared to 175 MΩ for the original alkanemonothiol network. The resistance change due to molecular exchange is considarably lower than found by Liao et al.[7], but close to the values found by the same group in ref. [8]. This discrepancy is probably due to an incomplete exchange reaction in our case. Nevertheless, the resistance change is large enough to conclude that transport is dominated by the OPE molecules. Figure 3.4 shows a bending experiment for an OPE-substituted sample, similar to the one in figure 3.2. We find that the network's resistance responds linearly to changes in Δy in the regime probed. The absolute resistance changes found are much smaller than for the alkanemonothiol networks. Moreover, also the relative resistance change $(R(\Delta d) - R(0))/R(0)$ has dropped significantly, from 0.34 ± 0.02 mm^{-1} for the initial network to 0.06 ± 0.01 mm^{-1} for the OPE-bridged sample. Since, apart from molecular insertion, the network itself is unchanged, we expect that $\Delta U/\Delta y$ and thus $\Delta d/\Delta y$ have the same values as for the original alkanemonothiol network (see equation 3.1). Hence, it is reasonable to state that the quantity $(\Delta R/R)/(\Delta d/d)$, i.e. the resistance response to strain, has dropped by a factor 0.34/0.06. In other words, the insertion of OPE-bridges has significantly changed the properties of our junctions, both in absolute resistance and in strain sensitivity. It is tempting to relate $(R(\Delta d) - R(0))/R(0)$ to the exponential factor 2κ, or more exactly, to the quantity β for the OPE-series. This

β-value is defined as the decay factor of conductance with molecular length L, for a series of oligomers [13, 16, 17]. However, we do not view this as the correct interpretation, since the OPE's are quite rigid rods compared to the relatively soft gold particles. It is more likely that the position of the molecule-Au connection changes upon straining the junction. For example, if the Au-thiol bond is initially near a step edge on the gold nanoparticle, it may jump over this edge to the upper gold layer upon pulling. Recently, Martin *et al.* argued that the latter configuration yields a higher resistance value [18].We note that the change of $(R(\Delta d) - R(0))/R(0)$ upon straining should then be seen as a statistical effect, i.e. as a result of shifting distributions in molecular anchoring. However we can also describe the results by assuming that the OPE3DT molecules do not bridge the NP's (see chapter 2). Indeed then the tunnel barrier is lowered by the presence of the OPE3 molecules.

We anticipate, however, that the situation will be very different for less rigid molecules. Especially spin transition molecules [19] are good candidates for future experiments, as they can be switched from a low-spin to a high-spin state when stretched[3]. In addition such molecules increase the certainty of the bridging (see chapter 2). Such measurements may be supported by surface enhanced Raman spectroscopy (SERS) studies, which would allow one to follow molecular vibrations as the junctions are strained.

3.6 Conclusions

In summary, we present a new method to statistically study molecular transport as a function of inter-electrode distance. Our platform combines the stability of 2D-molecular networks with the control of mechanically controllable break junctions with a maximal variation around 50 pm per junction. We demonstrate that both the absolute and relative resistance response depend on the molecular species present in the junctions. Hence, this study paves the road towards future experiments on strain-sensitive molecules. Moreover, using this technique, a strain sensor with tunable sensitivity can be considered.

References

[1] R. M. Metzger, *Unimolecular electronics*, Journal of Materials Chemistry **18**, 4364 (2008).

[2] S. J. van der Molen and P. Liljeroth, *Charge transport through molecular switches*, Journal Of Physics-Condensed Matter **22**, 133001 (2010).

[3] J. J. Parks, A. R. Champagne, T. A. Costi, W. W. Shum, A. N. Pasupathy, E. Neuscamman, S. Flores-Torres, P. S. Cornaglia, A. A. Aligia, C. A. Bal-

seiro, et al., *Mechanical Control of Spin States in Spin-1 Molecules and the Underscreened Kondo Effect*, Science **328**, 1370 (2010).

[4] N. Agrait, A. L. Yeyati, and J. M. van Ruitenbeek, *Quantum properties of atomic-sized conductors*, Physics Reports-Review Section Of Physics Letters **377**, 81 (2003).

[5] R. H. M. Smit, Y. Noat, C. Untiedt, N. D. Lang, M. C. van Hemert, and J. M. van Ruitenbeek, *Measurement of the conductance of a hydrogen molecule*, Nature **419**, 906 (2002).

[6] R. P. Andres, J. D. Bielefeld, J. I. Henderson, D. B. Janes, V. R. Kolagunta, C. P. Kubiak, W. J. Mahoney, and R. G. Osifchin, *Self-assembly of a two-dimensional superlattice of molecularly linked metal clusters*, Science **273**, 1690 (1996).

[7] J. H. Liao, L. Bernard, M. Langer, C. Schönenberger, and M. Calame, *Reversible formation of molecular junctions in two-dimensional nanoparticle arrays (vol 18, pg 2444, 2006)*, Advanced Materials **18**, 2803 (2006).

[8] L. Bernard, Y. Kamdzhilov, M. Calame, S. J. van der Molen, J. Liao, and C. Schönenberger, *Spectroscopy of Molecular Junction Networks Obtained by Place Exchange in 2D Nanoparticle Arrays*, journal of physical chemistry C **111**, 18445 (2007).

[9] S. J. van der Molen, J. H. Liao, T. Kudernac, J. S. Agustsson, L. Bernard, M. Calame, B. J. van Wees, B. L. Feringa, and C. Schönenberger, *Light-Controlled Conductance Switching of Ordered Metal-Molecule-Metal Devices*, Nano Letters **9**, 76 (2009).

[10] J. Slot and H. Geuze, *A new method for preparing gold probes for multiple labeling cytochemistry*, European Journal of cell biology **38**, 87 (1985).

[11] S. A. G. Vrouwe, E. van der Giessen, S. J. van der Molen, D. Dulic, M. L. Trouwborst, and B. J. van Wees, *Mechanics of lithographically defined break junctions*, Physical Review B **71** (2005).

[12] K. E. Mueggenburg, X. M. Lin, R. H. Goldsmith, and H. M. Jaeger, *Elastic membranes of close-packed nanoparticle arrays*, Nature Materials **6**, 656 (2007).

[13] H. B. Akkerman and B. de Boer, *Electrical conduction through single molecules and self-assembled monolayers*, Journal Of Physics-Condensed Matter **20** (2008).

[14] X. Y. Xiao, L. A. Nagahara, A. M. Rawlett, and N. J. Tao, *Electrochemical gate-controlled conductance of single oligo(phenylene ethynylene)s*, Journal Of The American Chemical Society **127**, 9235 (2005).

[15] H. Valkenier, E. H. Huisman, P. A. van Hal, D. M. de Leeuw, R. C. Chiechi, and J. C. Hummelen, *Formation of High-Quality Self-Assembled Monolayers of Conjugated Dithiols on Gold: Base Matters*, J. Am. Chem. Soc. **133**, 4930 (2011).

[16] N. J. Tao, *Electron transport in molecular junctions*, Nature Nanotech. **1**, 173 (2006).

[17] E. H. Huisman, C. M. Guedon, B. J. van Wees, and S. J. van der Molen, *Interpretation of Transition Voltage Spectroscopy*, Nano Letters **9**, 3909 (2009).

[18] M. N. Martin, J. I. Basham, P. Chando, and S. K. Eah, *Charged Gold Nanoparticles in Non-Polar Solvents: 10-min Synthesis and 2D Self-Assembly*, Langmuir **26**, 7410 (2010).

[19] R. Chandrasekar, F. Schramm, O. Fuhr, and M. Ruben, *An Iron(II) spin-transition compound with thiol anchoring groups*, European Journal Of Inorganic Chemistry pp. 2649–2653 (2008).